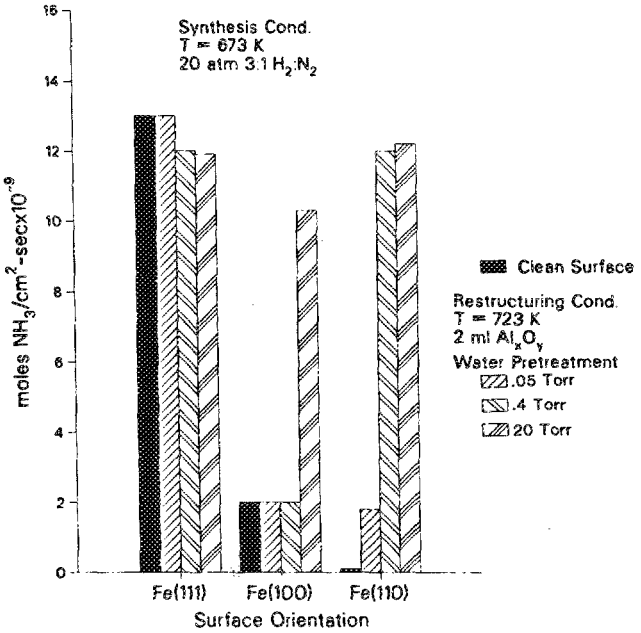

FIG. 1. Ammonia synthesis rates over clean iron single crystals and restructured Al_xO_y/Fe surfaces. A rate is given to the clean Fe(110) surface in this figure for clarity but in actuality the ammonia yield from this crystal face is below the detection limit of the PID (1×10^{-10} mol NH_3/cm^2 s).

sure. Aluminum was evaporated from a Knudsen-type cell and it was readily oxidized to Al_xO_y by leaking oxygen into the UHV chamber. Coverages of aluminum oxide were determined by carbon monoxide titrations[2,3] [one monolayer (ML) of Al_xO_y is defined as the point where no CO chemisorbs to the sample]. Rates of ammonia synthesis were corrected for the iron surface which was covered by aluminum oxide.

Figure 1 shows the rates of ammonia synthesis over the clean iron single crystals and restructured Al_xO_y (2 ML)/Fe surfaces after water vapor treatments were performed at 723 K for 30 min in the high-pressure cell (water vapor pressures are given in the figure). The most marked change in activity is in the case of the Al_xO_y/Fe(110) surface. After a 0.4-Torr water vapor treatment the initially inactive (110) surface becomes almost as active as the Fe(111) surface. The same change in rate can be achieved without aluminum oxide by using a 20-Torr water vapor treatment but the surface is transformed into the inactive (110) surface within 1 h of ammonia synthesis.

The activity of the (111) and (211) surfaces of iron is usually attributed to the presence of C_7 sites (iron atoms with seven nearest neighbors)[4,5] which can enhance the rate limiting step in the ammonia synthesis reaction (the dissociation of dinitrogen).[6] This suggests that through the water induced restructuring of Fe(110) and Fe(100), surface orientations which expose C_7 sites [i.e., Fe(111) and Fe(211)] are being created, but only in the presence of aluminum oxide are these new orientations stable under ammonia synthesis conditions.

Acknowledgment: This work was supported by the Director, Office of Energy Research, Office of Basic Energy Sciences, Materials Science Division of the U.S. Department of Energy Under Contract No. DE-AC03-76SF00098.

[1]N. D. Spencer, R. C. Schoonmaker, and G. A. Somorjai, J. Catal. **74**, 129 (1982).
[2]S. R. Bare, D. R. Strongin, and G. A. Somorjai, J. Phys. Chem. **90**, 4726 (1986).
[3]D. R. Strongin, S. R. Bare, and G. A. Somorjai, J. Catal. **103** (1987).
[4]J. A. Dumesic, H. Topsoe, and M. Boudart, J. Catal. **37**, 513 (1975).
[5]D. R. Strongin, J. C. Carrazza, S. R. Bare, and G. A. Somorjai, J. Catal. **102** (1986).
[6]P. H. Emmett, in *The Physical Basis for Heterogeneous Catalysis*, 3rd ed., edited by E. Drauglis and R. Jaffe (Plenum, New York, 1975).

Summary Abstract: The hydrogenolysis of alkanes over single-crystalline surfaces of iridium: The influence of surface structure on the catalytic selectivity

J. R. Engstrom[a] and D. W. Goodman
Surface Science Division, Sandia National Laboratories, Albuquerque, New Mexico 87185
W. H. Weinberg
Division of Chemistry and Chemical Engineering, California Institute of Technology, Pasadena, California 91125

(Received 13 October 1986; accepted 28 January 1987)

The study of the reactions of saturated hydrocarbons with hydrogen over transition-metal surfaces is of considerable technological importance, most notably to the hydroprocessing of petrochemical feedstocks. For many of these reactions, including alkane hydrogenolysis, the *specific* activity (per site basis) has been found to be sensitive to the average metallic particle size. This "structure sensitivity"[1] has been attributed to a number of effects which include variations in

TABLE I. Apparent rate parameters of hydrogenolysis reactions.[a]

Reaction	R(475 K)[b] (molecule site^{-1} s^{-1})	$k_{app}^{(c)}$ (molecule site^{-1} s^{-1})	E_{app} (kcal mol^{-1})
Ir(111) surface			
$C_3H_8 + H_2 \rightarrow CH_4 + C_2H_6$	1.0×10^{-2}	$4.7\times10^{13\pm1}$	33.5 ± 2
n-$C_4H_{10} + 2H_2 \rightarrow 2CH_4 + C_2H_6$	2.7×10^{-2}	$7.4\times10^{12\pm1}$	31.6 ± 2
Ir(110)-(1×2) surface			
$C_3H_8 + H_2 \rightarrow CH_4 + C_2H_6$	1.5×10^{-2}	$1.2\times10^{14\pm1}$	34.7 ± 2
n-$C_4H_{10} + H_2 \rightarrow 2C_2H_6$	7.8×10^{-2}	$1.1\times10^{9\pm1}$	22.2 ± 2

[a] Rate parameters were fit to the observed total conversion by utilizing the expression $R = k_{app}^{(c)} \exp(-E_{app}/k_B T)$. Reactant partial pressures were 1.0 Torr of hydrocarbon and 100 Torr of hydrogen. For these reaction conditions, the range of temperatures over which the rate parameters apply is approximately 400–500 K.

[b] Reaction rate is in terms of total conversion.

the electronic and/or geometric nature of the surface with particle size. Unfortunately, a complete *microscopic* understanding of the observed variations in catalytic properties with particle size has yet to emerge.

We have examined the hydrogenolysis of ethane, propane, n-butane, and neopentane on both the (111) and the (110)-(1×2) single-crystalline surfaces of iridium.[2] These two surfaces were chosen in order to investigate the relationship between surface structure and both catalytic activity and selectivity. For example, the (110)-(1×2) surface contains a large fraction (25%) of low-coordination-number [C_7 (Ref. 3)] edge atoms, whereas a perfect (111) surface contains no such atoms. Thus, if the ratio of the number of edge atoms to the number of (111) face (C_9) atoms influences the kinetics and/or mechanism of a particular reaction, then a comparison of the (110)-(1×2) and (111) surfaces should be decisive in quantifying the connection between catalytic activity and/or selectivity and the *local* surface structure.

The results obtained for the hydrogenolysis of n-butane over the two surfaces are especially provocative. A dramatic difference in selectivity is observed in the product distributions over the two surfaces, the (110)-(1×2) surface exhibiting a high selectivity for ethane production. The *major* reaction pathways on the two surfaces are n-$C_4H_{10} + 2H_2 \rightarrow 2CH_4 + C_2H_6$ on Ir(111) and n-$C_4H_{10} + H_2 \rightarrow 2C_2H_6$ on Ir(110)-(1×2). The specific activities and apparent kinetic rate parameters for these two reactions are given in Table I.

Previous studies employing supported Pt[4] and Ir[5] catalysts have indicated that the product distributions from n-butane hydrogenolysis are sensitive to the average metallic particle size. In particular, the selectivity for ethane increases dramatically as the particle size is decreased. Foger and Anderson[5] have reported that this structure sensitivity is most evident for Ir crystallites of diameter $\leqslant$40 Å, where there is a rapid variation in the average coordination number of the metal surface atoms.[6] In order to compare these results obtained with supported Ir catalysts of varying particle size to ours obtained over the Ir(111) and Ir(110)-(1×2) surfaces, we have computed an "effective particle size" for the single-crystalline surfaces utilizing the ratio of the number of edge (C_7) atoms to the number of (111) face (C_9) atoms as the appropriate criterion.[7] For instance, for the (110)-(1×2) surface, the ratio C_7/C_9 is $\frac{1}{2}$, whereas for the (imperfect) (111) surface employed here, we have estimated that the ratio is approximately $\frac{1}{20}$.[8] Assuming the supported catalyst particles form shapes of either octahedral or square-pyramidal (half-octahedral) structure, the calculated effective particle diameters are approximately 24 or 13 Å for the Ir(110)-(1×2) surface, and 166 or 81 Å for the Ir(111) surface, respectively.[9]

The selectivity for ethane production for both the supported catalysts[5] and the two single-crystalline surfaces are shown in Fig. 1 as a function of the mean particle diameter.

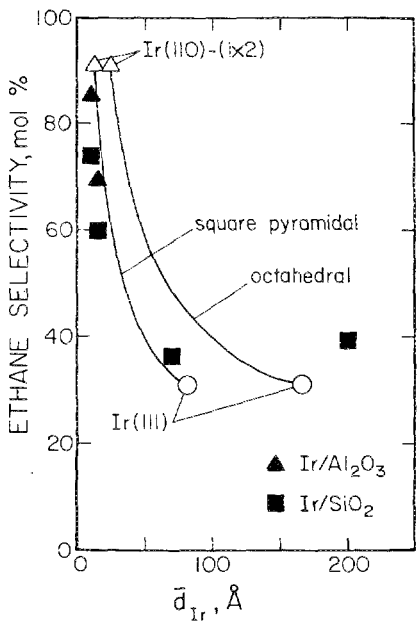

FIG. 1. Selectivity for ethane production (mol % of total products) from the hydrogenolysis of n-butane over Ir catalysts plotted as a function of the mean Ir particle size. Data for the supported catalysts are from Foger and Anderson (Ref. 5). The abscissas for the two single-crystalline surfaces were determined by a calculated effective particle size, as described in the text. The reaction temperature in all cases is 475 K. Note that for the reaction n-$C_4H_{10} + H_2 \rightarrow 2C_2H_6$, the selectivity for ethane is 100%, whereas for the reaction n-$C_4H_{10} + 2H_2 \rightarrow 2CH_4 + C_2H_6$, the selectivity for ethane is 33%.

The solid curves represent theoretical interpolations between the single-crystalline surfaces based on the geometrical shapes specified above. Obviously, there is an *excellent* correlation between the selectivity for ethane production and the mean Ir particle size. Based on our results, the observed increase in the ethane selectivity with decreasing particle size is identified clearly with the increasing participation of low-coordination-number C_7 surface atoms.

The profound differences in both the selectivity and the apparent activation energy of reaction (cf. Table I) that are observed for *n*-butane hydrogenolysis suggest strongly that different reaction mechanisms involving different intermediates are obtained on the two surfaces. Additional support for this proposal can be derived, e.g., by comparing these data for *n*-butane to those obtained for propane hydrogenolysis on the same two surfaces. The specific activities and apparent kinetic rate parameters for propane hydrogenolysis are displayed in Table I for comparison. The rate parameters for the hydrogenolysis of propane on both surfaces, and for *n*-butane on the Ir(111) surface are virtually identical, implicating similar reaction pathways. Moreover, for these three cases, the variations in the specific rates of reaction with changing reactant partial pressures are described well by a reaction mechanism involving irreversible C–C bond cleavage in a partially dehydrogenated adsorbed hydrocarbon fragment as the rate-limiting step.[2] However, *n*-butane hydrogenolysis over the Ir(110)-(1×2) surface is described poorly by this mechanism. Rather, a mechanism involving *reversible* C–C bond cleavage in a "symmetrical" adsorbed reaction intermediate provides a superior fit to the data.[2] The implicated stoichiometries of the reaction intermediates involved in the reversible C–C bond cleavage reaction are given by $C_4H_8(a) \rightleftharpoons 2C_2H_4(a)$. Based on both this implicated reaction mechanism and precedents from organometallic chemistry,[10,11] the most plausible structure for the parent hydrocarbon fragment, $C_4H_8(a)$, on the Ir(110)-(1×2) surface is a *metallacycle pentane*.

Supporting evidence for the metallacycle intermediate (implicitly *mono*nuclear) can be provided if one considers the stereochemistry of its formation on the two surfaces considered here. For example, utilizing bond lengths and bond angles from Ir[12] and Pt[13] homogeneous complexes containing metallacycle pentane ligands, one finds that significant repulsion is expected between the α-hydrogens and the adjacent Ir atoms on a (111) surface. However, no such repulsion is expected if one coordinates the ligand about the (implicated "active site") low-coordination-number C_7 atom on the (110)-(1×2) surface. Since these C_7 atoms are not present on a (111) surface, the absence of the mononuclear metallacycle pentane intermediate on Ir(111) can be explained purely on a stereochemical basis.

In conclusion, we have investigated the hydrogenolysis of various short-chain alkanes on the Ir(111) and Ir(110)-(1×2) surfaces. A striking correlation has been discovered between the selectivity for ethane production from the hydrogenolysis of *n*-butane over Ir catalysts and the concentration of low-coordination-number metal surface atoms. This result is best interpreted as a manifestation of the occurrence of a particular adsorbed reaction intermediate on the Ir(110)-(1×2) surface, namely, a metallacycle pentane. The formation of this intermediate is sterically forbidden on the Ir(111) surface.

Acknowledgments: This work was performed at Sandia National Laboratories and supported by the U. S. Department of Energy under Contract No. DE-AC04-76DP00789. We acknowledge the partial support of the Office of Basic Energy Sciences, Division of Chemical Science.

[a] Visiting from the Division of Chemistry and Chemical Engineering, California Institute of Technology, Pasadena, CA 91125.

[1] M. Boudart, Adv. Catal. **20**, 153 (1969).
[2] J. R. Engstrom, D. W. Goodman, and W. H. Weinberg (submitted for publication).
[3] R. van Hardeveld and F. Hartog, Adv. Catal. **22**, 75 (1972).
[4] (a) G. Leclercq, J. Trochet, and R. Maurel, C. R. Acad. Sci. Ser. C **276**, 1353 (1973); (b) L. Guczi and B. S. Gudkov, React. Kinet. Catal. Lett. **9**, 343 (1978).
[5] K. Foger and J. R. Anderson, J. Catal. **59**, 325 (1979).
[6] O. M. Poltorak and V. S. Boronin, Russ. J. Phys. Chem. **40**, 1436 (1966).
[7] J. R. Engstrom, D. W. Goodman, and W. H. Weinberg, J. Am. Chem. Soc. **108**, 4653 (1986).
[8] Hydrogen chemisorption data suggest the presence of approximately 2.5%–5.0% "defect sites" on this surface. See J. R. Engstrom, W. Tsai, and W. H. Weinberg (submitted for publication).
[9] These two geometrical shapes will bracket other probable regular polyhedra, e.g., cubo-octahedra or cubes.
[10] See, e.g., R. H. Grubbs and A. Miyashita, J. Am. Chem. Soc. **100**, 1300 (1978); R. H. Grubbs, A. Miyashita, M. Liu, and P. Burk, *ibid.* **100**, 2418 (1978).
[11] The importance of metallacycle pentanes in heterogeneous catalysis has been suggested previously, see, e.g., (a) G. Leclercq, L. Leclercq, and R. Maurel, J. Catal. **50**, 87 (1977); (b) A. F. Kane and J. K. A. Clarke, J. Chem. Soc. Faraday Trans. 1 **76**, 1640 (1980).
[12] (a) A. R. Fraser, P. H. Bird, S. A. Bezman, J. R. Shapely, R. White, and J. A. Osborn, J. Am. Chem. Soc. **95**, 597 (1973); (b) P. Diversi, G. Ingrosso, A. Lucheni, W. Porzio, and M. Zocchi, J. Chem. Soc. Chem. Commun. **1977**, 811.
[13] A. Cheethan, R. J. Puddephatt, A. Zalkin, D. H. Templeton, and L. K. Templeton, Inorg. Chem. **15**, 299 (1976).